AiMT Advances in Military Technology
Vol. 10, No. 2, December 2015

Study on Dynamic Performance of Armoured Vehicle in Lateral Direction due to Firing Impact

V. R. Aparow[1*], K. Hudha[1], M. M. Hamdan[1] and S. Abdullah[1]

[1]*Department of Mechanical, Faculty of Engineering, National Defense University of Malaysia, Kem Sungai Besi, 57000, Kuala Lumpur, Malaysia*

The manuscript was received on 11 May 2015 and was accepted after revision for publication on 11 December 2015.

Abstract:
This manuscript analysed the performance of 17 DOF wheeled armoured vehicle due to recoil force, in lateral direction. The vehicle model consisted of 7 DOF ride and handling, Pacejka Magic tire, 2 DOF Pitman Arm steering and 1 DOF gun turret models. A yaw moment occurred at the Centre of Gravity (CG) of the vehicle caused by the recoil force from gun. This recoil force creates instability conditions and affects the travelling path of the vehicle during firing. The vehicle model is evaluated using the firing angle of 45° and 90°, calibre size of 57 and 75 mm at speeds, 40 and 60 km/h. The vehicle model is evaluated in terms of yaw rate and angle, vehicle sideslip angle, lateral acceleration and displacement.

Keywords:

Armoured vehicle, firing recoil force, firing angle, lateral motion, yaw motion.

1. Introduction

According to Nato Reference Mobility Model, armoured fighting vehicle (AFV) is commonly recognized as a combat vehicle in the military application. The armoured vehicle is protected by extensive strong armour and also equipped with weapons such as the gun turret weapon platform on top of the vehicle [1, 2]. There are three priorities - firepower, mobility, and protection, also called the tank triangle which is mostly considered in main battle tanks design. These priorities were differently treated by different users, giving various approaches in armoured vehicle design [2, 3].

In order to increase the speed and mobility of armoured vehicles, many countries are starting to replace the tracked armoured vehicle with a wheeled type of armoured vehicles [4-6]. The wheeled armoured vehicles have cost-saving features where the development cost is considerably lower. Furthermore, wheeled armoured vehicles have a higher strategic and operational mobility, due to their lower weight. Thus, it increases

[*] *Corresponding author: Department of Mechanical, Faculty of Engineering, National Defense University of Malaysia, Kem Sungai Besi, 57000, Kuala Lumpur, +6014-9314908, E-mail: vimalrau87vb@gmail.com*

the strategic mobility, especially in term of air transportability, due to their lower weight than their tracked armoured vehicles [7]. Besides, the appearance of wheeled armoured vehicle is less aggressive than that of a tracked vehicle, which makes the wheeled armoured vehicle more suitable for peacekeeping operations [3,4].

Thus, wheeled armoured vehicle is one of the solutions to produce high mobility, better shooting and also scoot capabilities [8]. However, handling performance such as manoeuvrability of the wheeled armoured vehicle during gun firing has not been rigorously studied. The manoeuvrability of the armoured vehicles is significantly affected once an external disturbance from the gun turret platform is transferred to the armoured vehicle. The external disturbance due to recoil force from the gun turret while the vehicle is cruising at high speed causes the vehicle to drift out from its intended path. With this type of an emergency condition, lateral stability of armoured vehicles is highly difficult to be controlled only by a conventional steering wheel. Besides, low weight might cause lift-off, flip or slide over due to the external disturbance from a gun which acts in the lateral direction of the armoured vehicle [7].

A detailed research is required to evaluate the performance of the wheeled armoured vehicle before enhancing the performance in term of stability and mobility. Therefore, modelling and simulation tools are used as initial study by the previous automotive researchers to investigate the behaviour of the armoured vehicle. Previous researchers focused on the ride and stability system of a wheeled armoured vehicle by considering the longitudinal and vertical direction [5-8]. An armoured vehicle with 8 x 8 configurations is modeled with external disturbance of road and gun effect. However, the effect of armoured vehicles in lateral direction during gun firing has been neglected in these studies. The firing impact in lateral direction has been ignored by assuming the armoured vehicle performed firing in a static condition, not in a dynamic position.

Therefore, a detailed analysis on the performance of wheeled type armoured vehicle during firing is considered in this study. A light weight type of armoured fighting vehicle with a gun turret system is dealt with. Mathematical model which can be described as a 17 DOF armoured vehicle is used to investigate the performance of the armoured vehicle in lateral direction using a simulation tool, Matlab/SIMULINK. The 17 DOF model consists of 7 DOF ride model, 7 DOF handling model, Pacejka tire model, powertrain model and a 2 DOF Pitman Arm steering model. A single DOF of gun turret model was developed to introduce external disturbance to the armoured vehicle. Two types of calibres, 57 mm S-60 AAA (Russian gun) and 75 mm KwK 42 (Germany gun) have been chosen for this study based on the weight of the armoured vehicle. The performance of the armoured vehicle is evaluated during firing condition while traveling in longitudinal direction at the speed of 40 and 60 km/h.

This paper is organized as follows: The first section presents the introduction and review of some related works. The following section describes the modelling of the armoured vehicle dynamic behaviour in lateral direction. The next section discusses the effect of firing system on the armoured vehicle using two types of firing angle, 45° and 90° and calibres size, 57 mm and 75 mm at the constant vehicle speed of 40 km/h and 60 km/h. The final section is the conclusion of this paper.

2. The 17 DOF Armoured Vehicle Model

A 17 DOF wheeled armoured vehicle model using 4x4 configuration has been developed in this study using Newton's law of motions. The armoured vehicle model, has been developed using integration of few subsystems model to describe the behavior of an

armoured vehicle. The armoured vehicle model consists of the 7 DOF ride model, Pacejka Tire model, 7 DOF handling model, lateral and longitudinal slip model, 2 DOF Pitman arm steering model. A gun firing model has been included on top of the wheeled armoured vehicle to execute firing force which creates recoil force. The rotation of the gun turret model is demonstrated in *x-y* plane with one DOF [5].

2.1. Ride Model

The 7 DOF ride model is developed based on vertical force equations [5]. Tire vertical behavior is represented as a linear spring without damping while the wheel model has been developed with spring and damping system as shown in Fig. 1. The equation of the 7 DOF model is represented as follows

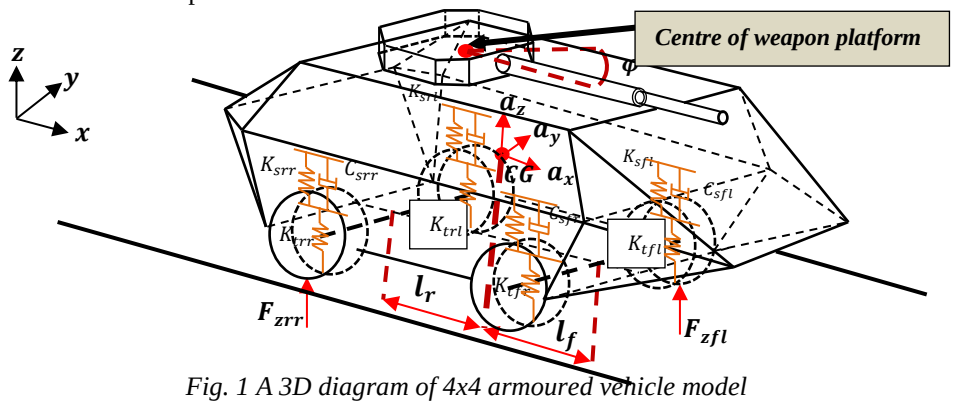

Fig. 1 A 3D diagram of 4x4 armoured vehicle model

$$F_{sfl}+F_{dfl}+F_{sfr}+F_{dfr}+F_{srl}+F_{drl}+F_{srr}+F_{drr} = m_b\ddot{z}_b \quad (1)$$

$$[F_{srl}+F_{drl}+F_{srr}+F_{drr}]l_r-[F_{sfl}+F_{dfl}+F_{sfr}+F_{dfr}]\,l_f = I_x\ddot{\emptyset}_p \quad (2)$$

$$[F_{sfl}+F_{dfl}+F_{srl}+F_{drl}]\frac{t}{2}-[F_{sfr}+F_{dfr}+F_{srr}+F_{drr}]\frac{t}{2} = I_y\ddot{\vartheta}_r \quad (3)$$

$$F_{tfl}-[F_{sfl}+F_{dfl}] = m_{wfl}\ddot{z}_{wfl}\ ;\ F_{tfr}-[F_{sfr}+F_{dfr}] = m_{wfr}\ddot{z}_{wfr} \quad (4)$$

$$F_{trl}-[F_{srl}+F_{drl}] = m_{wrl}\ddot{z}_{wrl}\ ;\ F_{trr}-[F_{srr}+F_{drr}] = m_{wrr}\ddot{z}_{wrr} \quad (5)$$

where F_{dfl}, F_{dfr}, F_{drl}, F_{drr}, F_{sfl}, F_{sfr}, F_{srl}, F_{srr}, F_{tfl}, F_{tfr}, F_{trl}, F_{trr} are the damper, spring and tire forces. Z_{wfl}, Z_{wfr}, Z_{wrl}, Z_{wrr} are the wheel displacement of the armoured vehicle. The detailed explanation of armoured vehicle ride model can be obtained from [5].

2.2. *Tire Model*

The tire model is one of the main components in obtaining both lateral and longitudinal motion of the armoured vehicle model. The tires provide lateral and longitudinal forces which contribute to the direction and speed of the armoured vehicle. The tire model included in this study is Pacejka Tire Model, developed as in [11] where an asphalt type of pavement is used. The lateral forces can be estimated using the Pacejka tire model based on the side slip angle of the armoured vehicle. Meanwhile, the longitudinal forces can be calculated by using longitudinal slip ratio. The general equation of the tire forces and moment is written as:

$$Y(X) = [y(x\ +\ S_h)] + S_v \quad (6)$$

where the value of S_h and S_v can be obtained using

$$S_h = (a_9\gamma_c)\,;\, S_v = [(a_{10}F_z^2) + (a_{11}F_z)] \times \gamma_c \quad (7)$$

The expression $y(x + S_h)$ represents the Pacejka Tire Model as follows:

$$y(x + S_h) = D \sin\left[C \arctan\left(B(x + S_h) - E(B(x + S_h) - \arctan B(x + S_h))\right)\right] \quad (8)$$

The term $Y(X)$ represents the value of cornering force, self-aligning torque or braking force. Meanwhile, the subscript *x* is used as the variable input such as slip angle, α (lateral direction) or slip ratio, λ (longitudinal direction) of each tires of the armoured vehicle and γ_c tire chamber angle. S_h and S_v represent the horizontal and vertical shift of the tire response, respectively. By substituting Eqs. (6-7) into Eq. (8), the lateral forces can be calculated using the side slip angle as the variable input. Likewise, the longitudinal slip ratio is used as input to obtain the longitudinal forces. The parameters *B*, *C*, *D* and *E* are defined as stiffness control, shape, peak and curvature factor. The equations are formulated using constant parameters a_1 to a_{11} which are obtained from experimental analysis for asphalt type pavement [11]. The responses of the lateral and longitudinal forces and self-aligning moment can be obtained as:

$$B = Stf/(CD) \quad (9)$$

$$D = (a_1F_z^2) + (a_2F_z) \quad (10)$$

$$E = (a_6F_z^2) + (a_7F_z) + a_8 \quad (11)$$

where Stf is defined as stiffness at zero slip, used to describe lateral force:

$$Stf = a_3 \sin(a_4 \arctan(a_5F_z)) \quad (12)$$

and, both longitudinal force and self-aligning moment as

$$Stf = [(a_3F_z^2) + (a_4F_z)]/e^{(a_5F_z)} \quad (13)$$

The parameter C is defined as 1.30 for lateral force, while for longitudinal force and self-aligning moment the parameters are 1.65 and 2.40. F_z referred to normal forces F_{zfl}, F_{zfr}, F_{zrl}, F_{zrr} at the tires of the armoured vehicle.

2.3. Handling Model

The handling model mainly describes the performance of armoured vehicle along the longitudinal *x*-axis, the lateral *y*-axis, and the rotational motion (yaw) about the vertical *z*-axis which contributes 3 DOFs. The motions are defined as a_x, a_y and $\ddot{r}$ respectively. Meanwhile, a single degree of freedom due to the rotational motion of each tire will contribute 4 DOF by the four tires. Hence, a total of 7 DOF will contribute to the performance evaluation of the armoured vehicle. Additionally, external disturbance such as drag forces, F_d and also the recoil force, F_{recoil} from gun turret weapon platform were also included in this model as shown in Fig. 2.

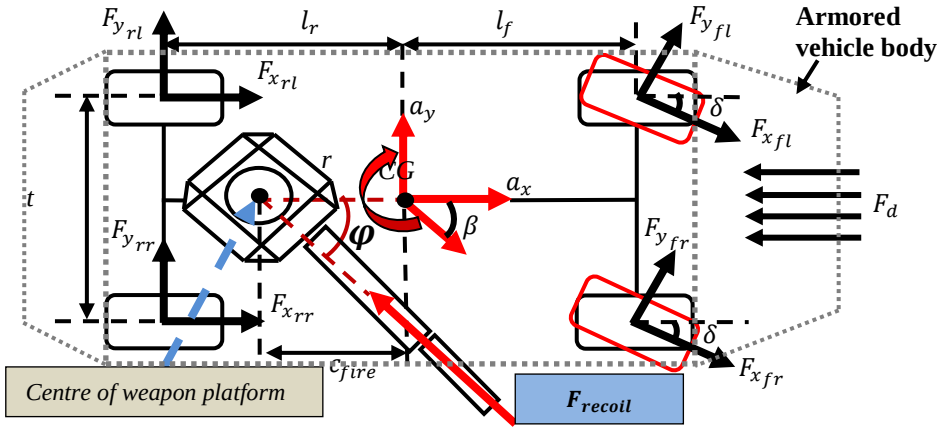

Fig. 2 A 2D diagram of 7 DOF Handling model of wheeled armoured vehicle

Summation of total forces acting on both lateral and longitudinal motion is mainly considered to formulate the lateral and longitudinal acceleration of the armoured vehicle. Besides, aerodynamic resistance which occurred at the front panel of the armoured vehicle and the backward momentum due to firing recoil force from the gun turret were also modelled in the total summation forces. The mathematical model of longitudinal force can be expressed as

$$\sum F_x = ma_x = F_{xrr} + F_{xrl} + (F_{yfr}+F_{yfl}) \sin \delta_f + (F_{xfr} + F_{xfl}) \cos \delta_f + \\ + (mg \sin \theta) - \Sigma F_d(v_x) + F_{recoil} \cos \varphi \quad (14)$$

where

$$\sum F_d(v_x) = F_a + F_r = \frac{1}{2} \rho A C_d v_x^2 + mgC_r v_x \quad (15)$$

Aerodynamic and rolling resistance, F_a, F_r are limited to the maximum linear speed of the armoured vehicle in longitudinal direction. The coefficient of the aerodynamic, C_d and rolling, C_r are 0.29 and 0.01. The lateral forces can be defined as

$$\sum F_y = ma_y = F_{yrr}+F_{yrl}+(F_{yfr}+F_{yfl}) \cos \delta_f - (F_{xfr} + F_{xfl}) \sin \delta_f - F_{recoil} \sin \varphi \quad (16)$$

Based on the lateral and longitudinal forces acting on all tires, the yaw acceleration, $\ddot{r}$, can be expressed using summation of moment method. In order to formulate the response, the centre of gravity (CG) of armoured vehicle is used as the reference point, thus

$$\sum M_{yaw} = I_z \ddot{r} = [F_{xrr}-F_{xrl}-(F_{yfr}-F_{yfl}) \sin \delta_f - (F_{xfr}-F_{xfl}) \cos \delta_f] \, t/2 + [F_{yrr}+F_{yrl}]l_r \\ +[-(F_{yfr} + F_{yfl}) \cos \delta_f + (F_{xfr}+F_{xfl} \sin \delta_f]l_f + [M_{z_{fl}}+M_{z_{fr}}+M_{z_{rl}}+M_{z_{rr}}] \\ +[(F_{recoil} \sin \varphi) \times c_{fire}] \quad (17)$$

where F_{xfr}, F_{xfl}, F_{xrr}, F_{xrl} F_{yfr}, F_{yfl}, F_{yrr}, M_{zrl}, M_{zfr}, M_{zfl}, M_{zrr} and M_{zrl} are the longitudinal force, lateral force and self-aligning moment of each tires at front right, front left, rear right and rear left of each tires respectively. The lateral and longitudinal accelerations always influenced by the yaw response acting at CG of the armoured vehicle. Thus, both acceleration responses can be formulated by considering the effect of yaw motion given by

$$\dot{v}_x = a_x + v_y\dot{r} \;\; ; \dot{v}_y = a_y + v_x\dot{r} \tag{18}$$

Using Eqs. (14) and (16), the vehicle body slip can be identified, denoted by β:

$$\beta = \arctan\left(\int_0^\infty \dot{v_y} / \int_0^\infty \dot{v_x}\right) \tag{19}$$

On the other hand, summation of reaction torques acting at each wheel has been formulated in order to obtain the angular speed of each wheel. The front and rear angular acceleration of the vehicle, $\dot{\omega}_{fl/fr}$ and $\dot{\omega}_{rl/rr}$, can be expressed as follows:

$$(I_{fi,j} \times \dot{\omega}_{fi,j}) = \tau_{e_{fi,j}} + \tau_{r_{fi,j}} - \tau_{b_{fi,j}} - \tau_{d_{fi,j}}(\omega_{fi,j}) \tag{20}$$

$$(I_{ri,j} \times \dot{\omega}_{ri,j}) = \tau_{r_{ri,j}} - \tau_{b_{ri,j}} - \tau_{d_{ri,j}}(\omega_{ri,j}) \quad ; i = \text{left}, j = \text{right} \tag{21}$$

where $I_{fi,j}$ and $I_{ri,j}$ are the mass of inertia of the front and rear wheels, $\tau_{e_{fi,j}}$ are the torques delivered by the engine to each front wheels only since the armoured vehicle is considered as a front wheel drive vehicle in this study therefore the rear wheel is assumed to be zero. Meanwhile, $\tau_{b_{fi,j}}$ and $\tau_{b_{ri,j}}$ are the brake torques applied to each front and rear wheels during braking input. The reaction torques at front and rear wheel, defined as $\tau_{r_{fi,j}}$ and $\tau_{r_{ri,j}}$, while the viscous friction torque are expressed $\tau_{d_{fi,j}}$ and $\tau_{d_{ri,j}}$. The detailed derivations of the terms are explained in [10].

2.4. Lateral and Longitudinal Slip Model

The lateral and longitudinal slips are used as input model in the tire model to obtain the lateral and longitudinal forces. The angle between tire direction of motion and the wheel plane is described as the lateral slip angle, α. The tire lateral slip angle at the front and rear tires can be derived as:

$$\alpha_{fi,j} = \arctan[(v_y + l_f\dot{r})/(v_x + (0.5t)\dot{r}] - \delta_f \tag{22}$$

$$\alpha_{ri,j} = \arctan[(v_y - l_f\dot{r})/(v_x + (0.5t)\dot{r}] \quad ; i = \text{left}, j = \text{right} \tag{23}$$

where, $\alpha_{fi,j}$ and $\alpha_{ri,j}$ are the lateral slip angles of tires at the front and rear of the vehicle. The wheel angle, δ_f, only affects the front lateral slip angle, α, since only the front wheel is steered via steering input. Meanwhile, the longitudinal slip of the tire is defined as the difference between the tire tangential velocity and the velocity of the axle relative to the road direction. The longitudinal slip, λ, as discussed in [10], described the effective coefficient of force transfer, which is obtained by measuring the difference between the longitudinal velocity of the vehicle, v_x, and the rolling speed of the tire, ωR, where R represents the radius of each wheel and ω, is the angular velocity of the wheel.

2.5. Development of Pitman Arm Steering Model

Three types of input models which are steering, powertrain and brake models are needed to describe the motion of armoured vehicle in lateral and longitudinal direction. The performance of the armoured vehicle in longitudinal motion is not observed in this study since there is no steering input while travelling in the longitudinal direction. Besides, the armoured vehicle is assumed to travel at constant speed where no braking input is applied. Therefore, the performance of the armoured vehicle in terms of wheel and vehicle speed and longitudinal slip for each wheel is not shown in the discussion. Meanwhile, the powertrain system has been discussed in detail in [10].

Pitman Arm steering system is commonly used in heavy vehicles especially wheeled armoured vehicle. Thus, a two DOF Pitman arm steering model was developed using Newton's second law of motion, based on the system as shown in Fig. 3. A few components in the mechanism need to be considered in the equation which is steering column itself, universal joint, hydraulic assisted pump, worm gear, sector gear and Pitman Arm. By assuming the rotation of steering wheel is equivalent to the rotational motion of steering column, then

$$I_{sc}\ddot{\theta}_{sc} + B_{sc}\dot{\theta}_{sc} + K_{sc}(\theta_{sc} - \theta_{sw}) = T_{HP} - T_{PA} - F_C \operatorname{sign} \dot{\theta}_k \tag{24}$$

where I_{sc}, B_{sc} and F_c is moment of inertia, viscous damping, friction of steering column. T_{HP} and T_{PA} are the torque due to hydraulic assisted pump and Pitman Arm. Meanwhile, θ_{sw}, θ_{sc} and θ_k are angular displacement of the steering wheel, column and universal joint respectively. Due to the limitation of space at the engine location of the heavy vehicle, the hydraulic power assisted system cannot be located at the same axis as the steering wheel [12]. Hence, an additional joint known as universal joint is used where it allows transmission of torque occurred between two non-parallel axes. This introduces a slight deviation in angle as shown in Fig. 4 represented by $\emptyset$ between two axes [12]. The angle of $\emptyset$ is set at 20 degree lower than the steering column [13], θ_{sc}. The angle θ_k is described by:

$$\theta_k = \arctan(\tan\theta_{sc}/\cos\emptyset) \tag{25}$$

The mechanism connected to the steering column is the hydraulic power assisted unit. This unit enables elimination of extensive modifications to the existing steering system and reduces effort by the driver to rotate the steering wheel since the hydraulic power assisted unit is able to produce large steering effort using hydraulic pump, rotary spool valve and Pitman Arm. The rotary spool valve consists of torsion bar, inner spool and also outer sleeve. Once input is applied to the steering wheel, it produces torque to twist the torsion bar and it rotates the inner spool with respect to the outer sleeve. This rotation tends to open the metering orifice hence increases the hydraulic fluid flow to actuate the worm gear. The hydraulic fluid flow through an orifice can be described:

$$Q_o = A_o C_{do}\sqrt{2\Delta P/\rho} \tag{26}$$

where, A_o and ΔP are cross sectional area and differential pressure of the orifice. Meanwhile, C_{do} = 0.6, is fluid flow coefficient and ρ is fluid density. The overall hydraulic power assisted equation can be derived by applying Eq. (28) as in Eq. (29).

$$Q_s + A_1 C_{do}\sqrt{2/(\rho\sqrt{|P_s - P_r|})} = (V_s/\beta_f)\dot{P}_s \tag{27}$$

Then, right and left cylinder pump pressure,

$$A_1 C_{do}\sqrt{2/(\rho\sqrt{|P_s - P_r|})} - A_2 C_{do}\sqrt{2/(\rho\sqrt{|P_r - P_o|})} - A_P\dot{y}_L = \left(A_p\left((L/2) + y_r\right)/\beta_f\right)\dot{P}_r \quad (28)$$

$$A_2 C_{do}\sqrt{2/(\rho\sqrt{|P_s - P_l|})} - A_1 C_{do}\sqrt{2/(\rho\sqrt{|P_l - P_o|})} + A_P\dot{y}_L = \left(A_p\left((L/2) - y_r\right)/\beta_f\right)\dot{P}_l \quad (29)$$

By using P_l and P_r from expression (28) and (29), the hydraulic torque can be estimated

$$T_{HP} = lA_p\left(\int \dot{P}_l - \int \dot{P}_r\right) \quad (30)$$

where l is defined as the steering arm length and the length is 0.2 m. The term L is the hydraulic cylinder length, A_1, A_2 and A_p are the metering orifice areas at right and left cylinder and the piston area. Meanwhile, P_s, P_r, P_l and P_o are the pressure in pump, right and left cylinder and return pressure is 0 bar.

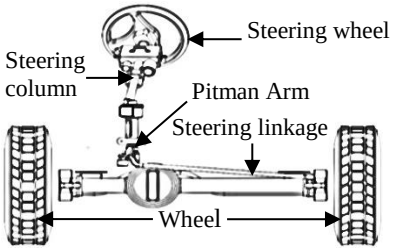

Fig. 3 Pitman arm steering system

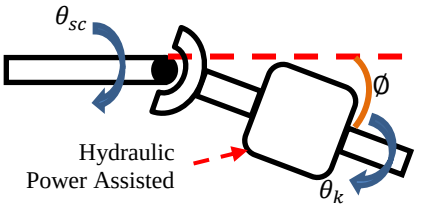

Fig. 4 Universal Joint at steering column

The output from the hydraulic power assisted model is connected to the worm gear which is directly connected to the sector gear and attached to a member link called Pitman Arm. The Pitman Arm converts the rotational motion of the steering column into translational motion at the steering linkage. The configuration of worm gear, sector gear and Pitman Arm member is shown in Fig. 5.

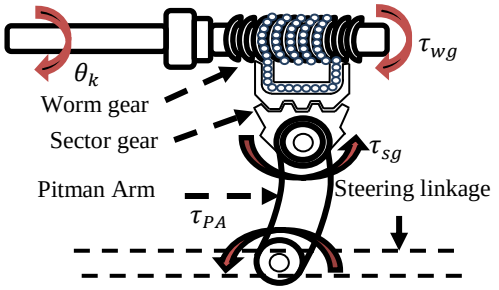

Fig. 5 System configuration using Pitman Arm

The output torque of the Pitman Arm link, τ_{PA}, can be obtained by equating both worm and sector gear as:

$$\tau_{wg} = K_{tr}(\theta_k - \theta_{wg}) \quad (31)$$

Since the torque created at sector gear is equal to the torque created at the end joint of Pitman Arm, hence

$$\tau_{sg} = \tau_{PA} = \eta_{sg}\tau_{wg} \tag{32}$$

where τ_{sg}, τ_{wg} are defined as the torque at sector and worm gear, while η_{sg} is the gear ratio at the sector gear. The rotational input from the sector gear is converted into translational motion to the steering linkage using Pitman Arm joint link. By using the torque from Pitman Arm as the input torque, the equation of motion of the steering linkage [14] is

$$M_L\ddot{y}_L + B_L\dot{y}_L + [C_{SL}\ \text{sign}(\dot{y}_L)] - [(b_r T_{PA})/(M_L R_{PA})] = \eta_f\ (T_{PA}/R_{PA}) - \eta_B(T_{KL}/N_M) \tag{33}$$

where M_L, B_L, C_{SL} are mass, viscous damping and coulomb friction breakout force of steering linkage. Additionally, the terms y_L, b_r, R_{PA} are the translational displacement, resistance at steering linkage and radius of Pitman Arm while η_f and η_B are gear ratio efficiency of forward and backward transmission respectively. By using Eq. (24), Eq. (30) and Eq. (34), the equation of motion of the wheel can be obtained. The output response of the wheel which is wheel angle, δ_f, is given by

$$I_{fi,j}\ddot{\delta_f} + B_{fw}\dot{\delta_f} + [C_{fw}\text{sign}\ (\dot{\delta_f})] = T_{KL} + T_a \tag{34}$$

and

$$T_{KL} = K_{SL}\ ((y_L/N_M) - \delta_f) \tag{35}$$

where B_{fw}, C_{FW} are the viscous damping of steering linkage bushing and coulomb friction breakout force on road wheel. T_a, T_{KL} are the tire alignment moment from Pacejka Magic Tire model and torque at steering linkage. The front wheel angle obtained from the 2 DOF Pitman Arm steering model is used in Eq. (14), Eq. (16), Eq. (17) and Eq. (22).

2.6. Development of Gun Firing Model

In order to evaluate the performance of the wheeled armoured vehicle due to the firing impact, a single degree of gun model was developed in this study. This model is located behind the CG of the armoured vehicle as shown in Fig. 1 and Fig. 2 and produced external force in the backward direction when firing towards a target. Various types of calibre projectile were used to evaluate the effect of recoil force to the armoured vehicle due to fire motion. The external force acting at the weapon platform can be formulated using Newton's law of motion [5]. A backward force known as an impulse is a vector unit to measure the effect of force acting on an object for a determinate amount of time.

The total backward impulse which is accumulated during recoiling process creates an external disturbance to the vehicle. This external disturbance caused the armoured vehicle to move out from its intended direction after firing. A burst type firing was used as recoil force by referring to [16]. The relationship of the recoil force of the projectile leaving a muzzle can be expressed as

$$\sum F_{recoil} = I_H/t_{FC} \tag{36}$$

where, I_H is the impulse of burst force depending on the ballistic properties and t_{FC} is defined as the time of functional cycle for each firing. The impulse of burst force is possible to calculate as the integral from the shot beginning to t_k shot final time [16]

$$I_H = \int_0^{t_k} F_H \, dt = [m_m + (\beta_g m_w)]v_0 \tag{37}$$

and,

$$\beta_g = (700 + v_0)/v_0 \tag{38}$$

where v_o is the initial velocity of the projectile leaving the muzzle, m_m and m_w are the mass of projectile and propellant charge while the factor of activity gunpowder gases is known as β_g [15]. The components of recoil forces acting at the weapon platform in the *x* and *y* directions depend on the firing angle (φ) in bearing direction only.

3. Description of Wheeled Armoured Vehicle

The wheeled armoured vehicle model describing the effect of recoil force of the gun model was developed based on the equations derived in sections 2.1 to 2.6 and simulated using MATLAB /SIMULINK software. The complete structure of the 9 DOF armoured is illustrated in Fig. 6. Two types of inputs which are steering and powertrain models are used to operate the armoured vehicle. Meanwhile, the gun model is used to introduce the external disturbance to the armoured vehicle due to backward momentum or recoil force.

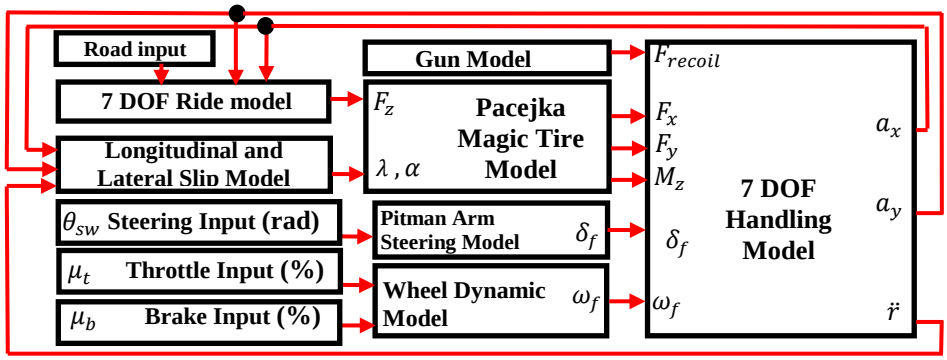

Fig. 6 Diagram of 4 x 4 wheeled armoured vehicle

4. Performance Evaluation of Armoured Vehicle

This section describes the dynamic performance in lateral direction of the wheeled armoured vehicle due to the gun recoil force. The armoured vehicle is assumed to move in a straight direction without initial steering input from the driver and performed attacks towards the target. Two types of calibres, 57 and 75 mm were used in the gun model to evaluate the effect of firing, since this vehicle is categorized as a light weight type of armoured vehicle [16]. This section begins by introducing the parameters used in the simulation study, followed by a presentation of the effect of armoured vehicle due to the firing recoil force using the two types of calibres and firing angles at the constant speed of 40 km/h and 60 km/h. The performance of the armoured vehicle is analysed in terms of dynamic performance in lateral motion such as yaw rate, yaw angle, vehicle sideslip, lateral acceleration and displacement.

4.1 Simulation parameters

The simulation was performed for a period of 5 seconds using Runge-Kutta solver with a fixed step size of 0.001 s. The numerical values of the 9 DOF wheeled armoured vehicle model parameters were set based on [5,14], while the gun model parameters are based on two types of guns with the calibre sizes of 57 mm S-60 AAA [17] and 75 mm KwK 42 [18] as shown in Tabs. 1, 2 and 3:

Tab. 1 Parameter of vehicle model

Description	**Symbol**	**Value**
Inertia of front and rear wheel	$I_{fi,j}$ and $I_{ri,j}$	15 kg. m^2
Vehicle mass	m_b	4210 kg
Wheel mass	$m_{wfl}, m_{wfr}, m_{wrl}, m_{wrr}$	50 kg
Tire radius	R_w	0.47 mm
Rear length from COG	l_r	2230 mm
Front length from COG	l_f	1070 mm
Vehicle width	t	1900 mm
Pitch Inertia	I_x	5000 kg. m^2
Roll Inertia	I_y	4300 kg. m^2
Yaw inertia	I_z	4700 kg. m^2
Tire spring stiffness	$K_{tfl}, K_{tfr}, K_{trl}, K_{tfr}$	100000 Nm
Suspension damper stiffness	$C_{sfl}, C_{sfr}, C_{srl}, C_{sfr}$	8000 Nm.s^{-1}
Suspension spring stiffness	$K_{sfl}, K_{sfr}, K_{srl}, K_{sfr}$	25000 Nm
Centre of gun turret	c_{fire}	0.35 m

Tab. 2 Parameter of gun model

Type	**57mm**	**75 mm**
v_o	1100 m/s	925 m/s
t_{FC}	0.25 s	0.25 s
m_m	2.85 kg	6.80 kg
m_w	1.18 kg	2.41 kg

Tab. 3 Parameter of Pitman arm steering model

Description	**Symbol**	**Value**
Moment of inertia of steering wheel	I_{sc}	0.035 kg m^2
Viscous damping of steering wheel	B_{sc}	0.36 Nm/(rad/sec)
Steering column rotational stiffness	K_{sc}	42000 Nm/rad
Pump flow rate	Q_s	0.0002 m^3/s
Piston area	A_p	0.005 m^2
Cylinder length	L	0.15 m
Fluid density	ρ	825 kg/m^3
Fluid volume	V_s	8.2× 10^{-5} m^3
Fluid bulk modulus	β_f	7.5× 10^8 N/m^2
Torsion bar rotational stiffness	K_{tr}	35000 Nm/rad
Moment of inertia of steering column	I_{sc}	0.055 kg m^2
Viscous damping of steering column	B_{sc}	0.26 Nm/ (rad/sec)
Coulomb friction breakout force	C_{SL}	0.5 N
Steering rotational stiffness	K_{SL}	15500 Nm/rad
Metering orifice	A_1	2.5 mm^2

4.2 Simulation Results

The simulation results show the effect of gun recoil force which was applied at t = 1.5 s at the bearing angle of 45° and 90°. From Fig. 13, it can be observed that maximum recoil up for 75 mm calibre is 41 kN at 90° and 29 kN at 45° while for 57 mm calibre it is 21 kN at 90° and at 45°, 15 kN are used since this vehicle is a light weight armoured vehicle. Besides, this vehicle is categorized as wheeled type of armoured vehicle, thus the contact point of the wheels and ground is lesser compared with the tracked vehicle. Therefore, an external force higher than the weight of the armoured vehicle might cause a roll-over or damage of the vehicle. Since the firing was performed in dynamic conditions, two types of constant speeds, 40 km/h and 60 km/h were used for both firing angles of 45° and 90°.

(a) Vehicle speed at 40 km/h

At a constant speed of 40 km/h of the armoured vehicle, recoil force was generated at the firing angles of 45° and 90°. As shown in Figures 7 and 8, for the firing angle of 45°, the recoil force using 75 mm calibre has produced the yaw rate up to 0.085 rad/s and 0.026 rad of yaw angle, while for 90° of the firing angle, the yaw rate and yaw angle increased to 0.135 rad/s and 0.041 rad. Meanwhile, the firing angle of 45° using 57 mm calibre produced 0.045 rad/s of yaw rate and 0.02 rad of yaw angle and at 90°, the yaw rate is 0.05 rad/s and 0.025 rad of yaw angle. The firing angle at 45 ° and 90° increased the unwanted deflection angle of the armoured vehicle. This unwnated deflection angle causes the armoured vehicle forced to travel outside of its intended path after the firing condition. Therefore, it can be observed that after firing at 45°, the armoured vehicle deviates from its initial position up to 1.1 m and 0.47 m for both 75 and 57 mm calibres. The displacement has increased gradually to 1.3 m and 0.48 m for both 75 and 57 mm calibres, once the firing angle increased to 90°, as shown in Fig. 10.

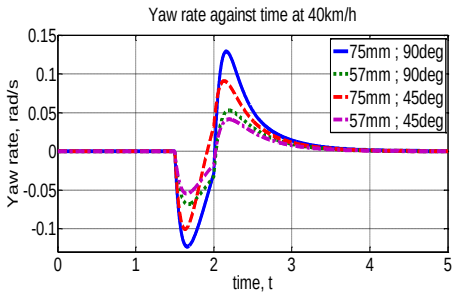

Fig. 7 Yaw rate against time

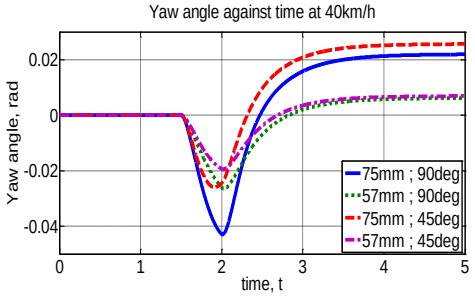

Fig. 8 Yaw angle against time

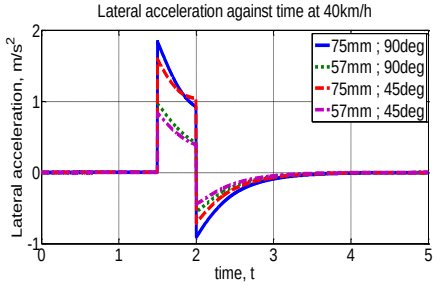

Fig. 9 Lateral acceleration against time

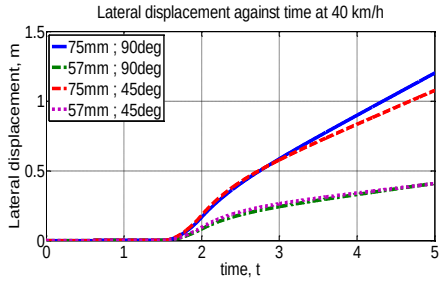

Fig. 10 Lateral displacement against time

(b) Vehicle speed at 60 km/h

Once the speed of the armoured vehicle is increased up to 60 km/h, the impact of firing recoil force has effected the dynamic performance of the armoured vehicle. According to Fig. 11 and Fig. 12, the firing force at 45° using 75 and 57 mm calibre has achieved maximum responses of yaw rate up to 0.11 and 0.051 rad/s. Meanwhile, the yawing angle has increased up to 0.04 and 0.028 rad. On the other hand, firing at 90° has amplified the effect by 80 to 85 % compared with previous firing angle where yaw rates are 0.18 and 0.075 rad/s for both 75 and 57 mm. Yaw angle, in addition, has also increased up to 0.061 and 0.039 rad. The increment of the vehicle speed from 40 km/h to 60 km/h have greatly increased the disturbance to the armoured vehicle. Similarly, the lateral displacement response is increased significantly where the vehicle is observed to deviate 1.35 m and 0.49 m out of its initial direction after firing action at 45° using 75 mm and 57 mm calibres, respectively.

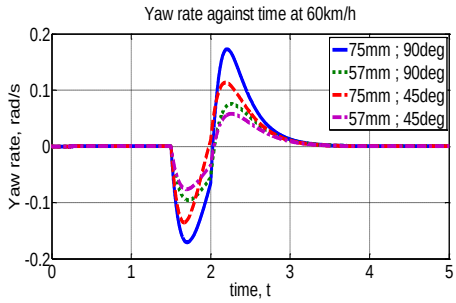

Fig. 11 Yaw rate against time

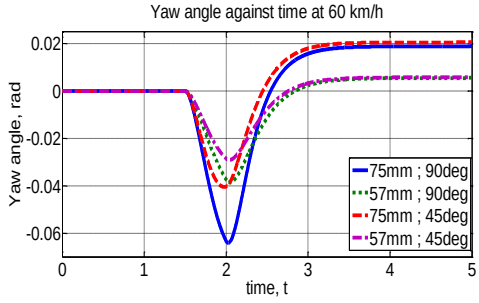

Fig. 12 Yaw angle against time

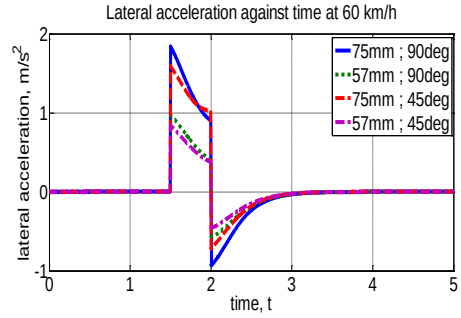

Fig. 13 Lateral acceleration against time

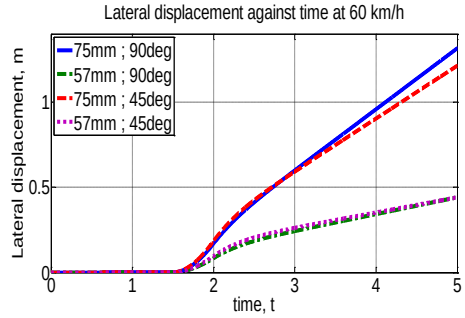

Fig. 14 Lateral displacement against time

Once the firing angle is increased to 90°, the lateral displacement has increased by 23 % from the initial position where the lateral displacements show 0.49 m and 1.43 m for 57 and 75 mm calibres as shown in Fig. 14. Based on the analysis, the firing force using 75 mm calibre produced a higher impact on the armoured vehicle. Thus, this response is used to validate the model with an actual firing test using 4x4 armoured vehicle at 60 km/h as shown in Figs. 15-18.

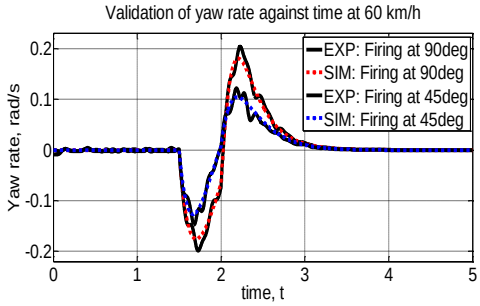

Fig. 15 Yaw rate against time

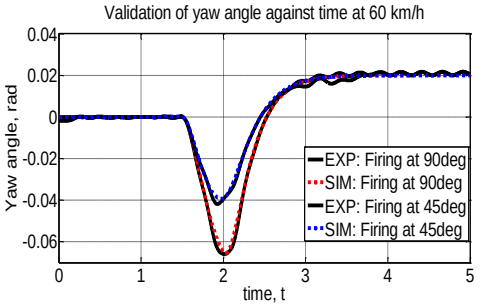

Fig. 16 Yaw angle against time

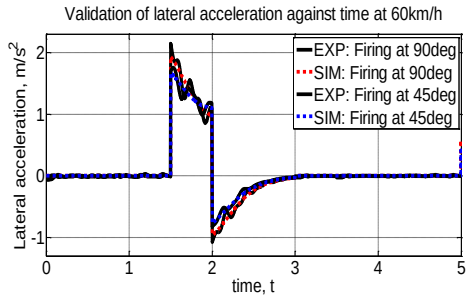

Fig. 17 Lateral acceleration against time

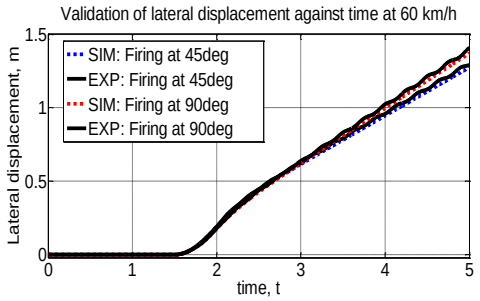

Fig. 18 Lateral displacement against time

Two types of sensors which are gyro and accelerometer are used to measure the response of the armoured vehicle. The sensors installed in the armoured vehicle during the testing procedure are shown in Fig. 19. Based on these results, the trends between simulated and actual armoured vehicle shows good agreement where by the response of the simulation model are almost similar with the experimental results during firing. This small fluctuation occurred in the actual results may be due to the flexibility of the armoured vehicle body which was neglected in the simulation model.

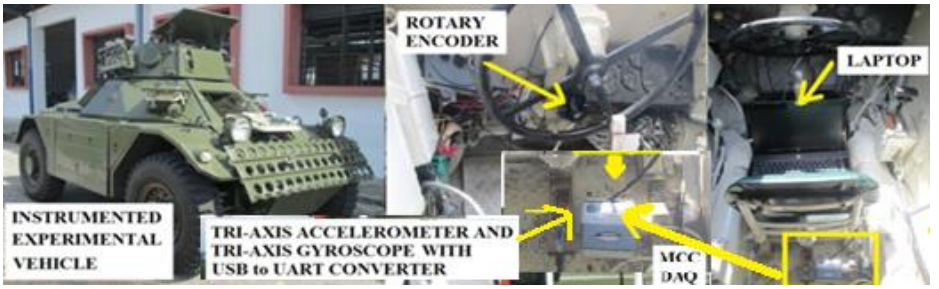

Fig. 19 Instrumented armoured vehicle

It can be observed that the performance of an armoured vehicle in the lateral direction is significantly affected by the firing force while performing the firing in dynamic position. Besides, using a larger projectile calibre and higher firing angle have increased the impact oo the armoured vehicle. It shows that the large backward force acting in the direction perpendicular to the side wall of armoured vehicle body creates a maximum firing moment at the CG of the armoured vehicle. Besides, the effects are gradually increased once the armoured vehicle is in motion. In order to avoid the effect,

most of the wheeled type armoured vehicle performed the firing in static position, not in dynamic condition. However, this situation increased the possibilities of the armoured vehicle to be targeted by the enemies for a counterattack [19].

5. Conclusion

In this study, it can be observed that the gun recoil force has reduced the dynamic performance of the armoured vehicle in lateral motion and that it affects the direction path of the armoured vehicle. Increasing the firing angle and calibre while in dynamic condition, results in the effect of the gun recoil force to the armoured vehicle. Thus, it can be concluded that firing in dynamic condition introduced unwanted disturbance to the armoured vehicle in lateral direction. As a solution, an active safety system is required to minimize the unwanted yaw disturbance due to the firing force and re-coordinate back the armoured vehicle to its travelling direction after the firing.

Acknowledgment

This work is part of a research project entitled “Robust Stabilization of Armored Vehicle Firing Dynamic Using Active Front Wheel Steering System”, funded by LRGS grant (No. LRGS/B-U/2013/UPNM/DEFENSE & SECURITY – P1) and led by Associate Professor Dr. Khisbullah Hudha. The authors would like to thank the Malaysian Ministry of Science, Technology and Innovation (MOSTI), MyPhD programme from Minister of Education and National Defense Universiti of Malaysia (NDUM) for their continuous support and the support is gratefully acknowledged.

References

[1] VONG, TT., HAAS, GA. and HENRY, CL. *NATO reference mobility model (NRMM) modeling of the Demo III experimental unmanned ground vehicle (XUV)* (No. ARL-MR-435). Army research lab aberdeen proving ground md.

[2] SCHMITT, V., RENOU, C. and GUIGUEN, N. French Study Program to Improve Active and Passive Safety on Military Vehicles. In *Proceedings: International Technical Conference on the Enhanced Safety of Vehicles*, 1999, Vol. 2005, National Highway Traffic Safety.

[3] BALOS, S., GRABULOV, V. and SIDJANIN, L. Future armoured troop carrying vehicles. *Defence Science Journal*, 2010, vol. 60, no. 5, p. 483-490.

[4] SOSNOWICZ, R., WACHOWIAK, P. and DORCZUK, M. *Conception of military vehicle classification*. Journal of KONES, 2011, vol. 18, p. 585-594.

[5] HUDHA, K., JAMALUDDIN, H. and SAMIN, P.M. *Disturbance rejection control of a light armoured vehicle using stability augmentation based active suspension system*. International Journal of Heavy Vehicle Systems 2008, vol. 15, no. 2, p. 152-169.

[6] TRIKANDE, MW., JAGIRDAR, VV. and SUJITHKUMAR, M. *Modelling and Comparison of Semi-Active Control Logics for Suspension System of 8x8 Armoured Multi-Role Military Vehicle*. Applied Mechanics and Materials, 2014, vol. 592, p. 2165-2178.

[7] YEAN, T. C., HONG, M. S. and YEW, V. *Fighting Vehicle Technology*. DSTA Horizons, 2013, p. 62-77.

[8] TVAROZEK, J. and GULLEROVA, M. Increasing Firing Accuracy of 2A46 Tank Cannon Built-in T-72 MBT. *American International Journal of Contemporary Research*, 2012, vol. 2, no. 9, p. 140-156.

[9] HUDHA, K., KADIR, Z. A. and JAMALUDDIN, H. Simulation and experimental evaluations on the performance of pneumatically actuated active roll control suspension

system for improving vehicle lateral dynamics performance. *International Journal of Vehicle Design*, 2014, vol. 64, no. 1, p. 72-100.

[10] APAROW, V. R., AHMAD, F., HUDHA, K. and JAMALUDDIN, H. Modelling and PID control of antilock braking system with wheel slip reduction to improve braking performance. *International Journal of Vehicle Safety*, 2013, vol. 6, no. 3, p. 265-296.

[11] WONG, J. Y. *Theory of ground vehicles*. John Wiley and Sons, 2001, p. 58-65.

[12] LIU, SC. Force feedback in a stationary driving simulator. *Systems, Man and Cybernetics, International Conference on IEEE*, Vancouver, BC, 22-25 October, 1995; p. 1711-1716.

[13] KARNOPP, D., ARGOLIS, R. and ROSENBERG, R. *System dynamis: modeling and simulations of mechatronic systems*, New York, 2000, NY: John Wiley Sons.

[14] SHWETHA, GN., RAMESH, HR. and SHANKAPAL, SR. Modeling, simulation and implementation of a proportional-derivative controlled column-type EPS. *International Journal of Enhanced Research in Science Technology and Engineering*, 2013, vol. 2, no. 9, p. 10-19.

[15] BORKOWSKI, W., FIGURSKI, J. and WALENTYNOWICZ, J. The impact of the cannon on the combat vehicle chassis during firing. *Journal of KONES*, 2007, vol. 14, p. 49-61.

[16] BALLA, J. Dynamics of mounted automatic cannon on track vehicle. *International Journal of Mathematical models and methods in applied sciences*, 2011, vol. 5, no. 3, p. 423-432.

[17] KOLL, C. *SOVIET CANNON - A Comprehensive Study of Soviet Guns and Ammunition in Calibres 12.7 mm to 57 mm*, 2009, ISBN 978-3-200-01445-9.

[18] *Germany's 75 mm Gun*, [cited 2015-08-15]. Available from: <http://www.wwiivehicles.com/ germany/guns/75-mm.asp>

[19] HUDHA, K., APAROW, VR., MURAD, M., ISHAK, SAF., KADIR, ZA., AMER, NH. And RAHMAN, MLHA. *Yaw Stability Control System*, Malaysian Patent, 14 October 2014, PI 2015700778.